Stem Cell Reports
Article

ISSCR

OPEN ACCESS

Regulation of Prostate Development and Benign Prostatic Hyperplasia by Autocrine Cholinergic Signaling via Maintaining the Epithelial Progenitor Cells in Proliferating Status

Naitao Wang,[1,4] Bai-Jun Dong,[2,4] Yizhou Quan,[1] Qianqian Chen,[1] Mingliang Chu,[1] Jin Xu,[1] Wei Xue,[2] Yi-Ran Huang,[2] Ru Yang,[1,5,*] and Wei-Qiang Gao[1,3,5,*]

[1]State Key Laboratory of Oncogenes and Related Genes, Renji-Med X Clinical Stem Cell Research Center, Ren Ji Hospital, School of Biomedical Engineering, Shanghai Jiao Tong University, Shanghai 200127, China
[2]Department of Urology, Renji Hospital, School of Medicine, Shanghai Jiao Tong University, Shanghai 200127, China
[3]Collaborative Innovation Center of Systems Biomedicine, Shanghai Jiao Tong University, Shanghai 200240, China
[4]Co-first author
[5]Co-senior author
*Correspondence: yangru@yahoo.com (R.Y.), gao.weiqiang@sjtu.edu.cn (W.-Q.G.)
http://dx.doi.org/10.1016/j.stemcr.2016.04.007

SUMMARY

Regulation of prostate epithelial progenitor cells is important in prostate development and prostate diseases. Our previous study demonstrated a function of autocrine cholinergic signaling (ACS) in promoting prostate cancer growth and castration resistance. However, whether or not such ACS also plays a role in prostate development is unknown. Here, we report that ACS promoted the proliferation and inhibited the differentiation of prostate epithelial progenitor cells in organotypic cultures. These results were confirmed by ex vivo lineage tracing assays and in vivo renal capsule recombination assays. Moreover, we found that M3 cholinergic receptor (*CHRM3*) was upregulated in a large subset of benign prostatic hyperplasia (BPH) tissues compared with normal tissues. Activation of CHRM3 also promoted the proliferation of BPH cells. Together, our findings identify a role of ACS in maintaining prostate epithelial progenitor cells in the proliferating state, and blockade of ACS may have clinical implications for the management of BPH.

INTRODUCTION

Regulation of proliferation and differentiation of prostate epithelial progenitor cells is important for the prostate development process of branching morphogenesis and prostate diseases. In the normal prostate, there are three epithelial cell types: basal cells ($p63^+$ and $CK5^+$), luminal cells ($CK8^+$), and neuroendocrine cells ($Synapthophysin^+$) (Leong et al., 2008). Even though several studies have identified the multipotent potential of luminal cells under castration conditions (Wang et al., 2009), in organoid cultures or in renal capsule recombination assays (Chua et al., 2014; Karthaus et al., 2014), it is also believed that multipotent epithelial progenitor cells are located in the basal cell compartment (Goldstein et al., 2010; Lawson et al., 2007; Leong et al., 2008; Ousset et al., 2012), which can differentiate into not only basal cells but also luminal cells and neuroendocrine cells. Previous studies, including the work from our group (Shou et al., 2001; Wang et al., 2003, 2006b, 2008), have shown that various signaling pathways can regulate epithelial progenitor cell proliferation and differentiation and, in turn, affect the formation of prostate diseases (Shen and Abate-Shen, 2010). However, whether or not there are additional important molecules that regulate prostate epithelial progenitor cells is still unclear.

Muscarinic receptors belong to the family of G-protein coupled receptors. There are five members: CHRM1–CHRM5 (Spindel, 2012). Activation of muscarinic receptors by acetylcholine usually stimulates Ca^{2+} influx, glandular secretion, and smooth muscle contraction (Wessler and Kirkpatrick, 2012). It was traditionally believed that acetylcholine was predominantly synthesized in the neuronal system. However, besides the neuronal cholinergic system, there is also a widespread cholinergic system in non-neuronal tissues, which has been identified in airway epithelial cells, hematopoietic stem cells, small intestine epithelial cells, colon epithelial cells, mesenchymal stem cells, and embryonic stem cells (Wessler and Kirkpatrick, 2012). The non-neuronal cholinergic signaling functions in regulating the differentiation and proliferation of embryonic stem cells (Landgraf et al., 2010), hematopoietic stem cells (Serobyan et al., 2007), and small intestine stem cells (Takahashi et al., 2014). In particular, our previous study demonstrated a role of autocrine cholinergic signaling (ACS) in promoting prostate cancer growth and castration resistance (Wang et al., 2015b). However, whether or not such ACS also plays a role in regulating proliferation and differentiation of prostate epithelial progenitor cells is unknown.

In the present study, we discovered the existence of ACS in the developing mouse epithelium. We used an organotypic culture system, which is free of functional nerve fibers, to study the roles of ACS in regulating prostate development. We further confirmed the results by lineage tracing and renal capsule tissue recombination assay. We

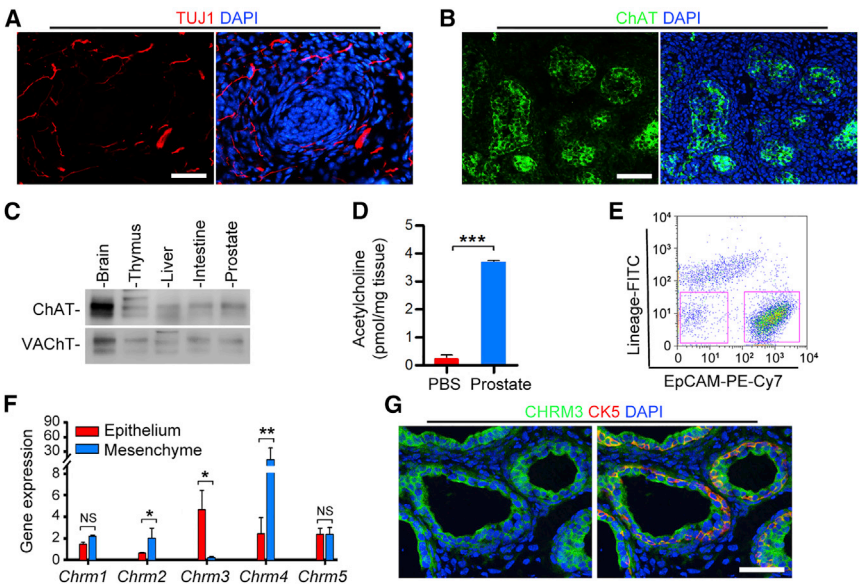

Figure 1. Prostate Epithelial Cells Express Cholinergic Markers and Release Non-neuronal Acetylcholine

(A) Immunostaining of TUJ-1 (red) in P5 mouse VP sections showing lack of nerve fibers in epithelial tissues. Scale bar, 50 μm.

(B) Immunofluorescent images showing epithelium-specific expressing of ChAT (green) in P5 mouse VP tissue sections. Scale bar, 100 μm.

(C) Western blotting analysis of ChAT and VAChT proteins in various mouse tissues.

(D) Fluorometric detection of acetylcholine in P5 mouse VPs after 2 days culture ex vivo (n = 3 experiments).

(E) Fluorescent-activated cell sorting of Lin^-EpCAM^+ epithelial cells and Lin^-EpCAM^- mesenchymal cells.

(F) Real-time PCR analysis of *Chrm1-Chrm5* levels in P5 mouse epithelial cells and mesenchymal cells (n = 3 experiments).

(G) Immunofluorescent staining of CHRM3 (green) and CK5 (red) in developing mouse VPs. Scale bar, 50 μm.

Data above were analyzed with Student's t test. *p < 0.05, **p < 0.01, ***p < 0.001. Error bars indicate SEM.

found that activation of ACS promoted prostate development by enhancing the proliferation of epithelial progenitor cells and preventing these progenitor cells from differentiation. In addition, we demonstrated that these effects were achieved through Ca^{2+}/calmodulin signaling, which could be blocked or reversed by a specific calmodulin inhibitor, W-7. More importantly, we found that *CHRM3* was upregulated in a large subset of BPH tissues compared with normal tissues. ACS promoted BPH cell proliferation through Ca^{2+}/calmodulin-signaling-mediated phosphorylation of AKT. Taken together, our findings identify ACS as another important component that keeps prostate epithelial progenitor cells in the proliferating state, and blockade of ACS may have clinical implications for the management of BPH.

RESULTS

Existence of ACS in the Developing Mouse Prostate Epithelium

Our previous study demonstrated the existence of functional ACS in regulating prostate cancer growth and castration resistance (Wang et al., 2015b). However, whether there is also an ACS in developing prostate epithelium and how this ACS regulates prostate development has not been determined. To examine the expression of cholinergic components in developing prostates, we performed immunofluorescent staining of TUJ-1 (a specific neuronal lineage marker) and ChAT (choline acetyltransferase, a key enzyme for the synthesis of acetylcholine) in P5 mouse ventral prostate (VP) sections. While a substantial number of TUJ-1 immunoreactive nerve fibers were observed in the mesenchyme, no nerve fiber was seen inside the epithelium (Figure 1A). In sharp contrast, epithelial cells were strongly immunoreactive for ChAT, a key enzyme responsible for the synthesis of acetylcholine (Figure 1B). In addition, western blotting analysis confirmed the expression of ChAT and vesicular acetylcholine transporter (VAChT) in postnatal mouse VPs (Figure 1C). Furthermore, we performed a fluorometric analysis to measure the synthesis of acetylcholine in isolated mouse VPs. We found that the isolated VPs could secrete acetylcholine after 2 days in cultures (Figure 1D). Since the parasympathetic nerve fibers were cut off during the dissection of VPs, most of the nerve fibers had degenerated and lost their functions after 2 days in culture (Figures S1A and S1B). Therefore, the acetylcholine was synthesized and secreted by prostate epithelial cells rather than from the nerve endings.

Activation of ACS needs not only the non-neuronal acetylcholine, but also the expression of muscarinic receptors in prostate epithelial cells. To examine the expression of muscarinic receptors in developing mouse prostate, we sorted prostate epithelial cells ($lineage^-EpCAM^+$) from mesenchymal cells ($lineage^-EpCAM^-$) by fluorescence-activated cell sorting (FACS) (Figure 1E) and measured the expression of muscarinic receptors, *Chrm1-Chrm5*. Real-time PCR analysis indicated that all five subtypes of muscarinic receptors are expressed in the prostate epithelial cells. While *Chrm2* and *Chrm4* were expressed at higher levels in the mesenchymal cells than in the epithelial cells (Figure 1F), expression levels of *Chrm1* and *Chrm5* did not

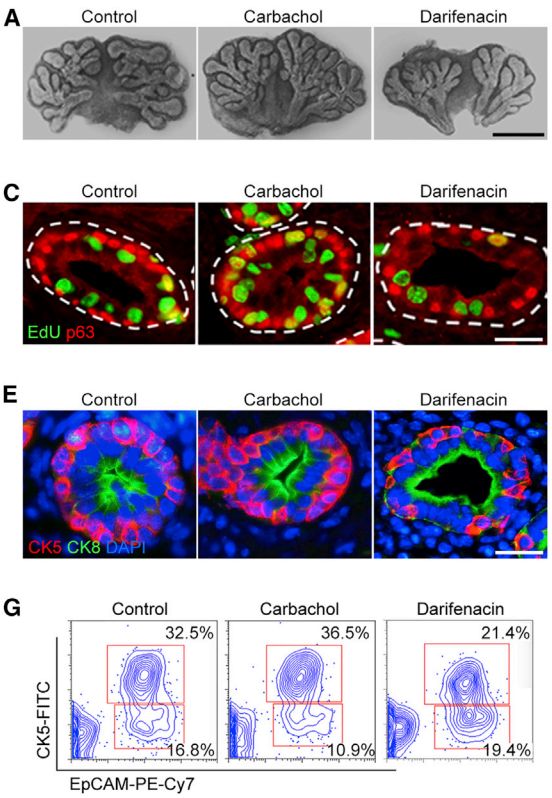

Figure 2. ACS Regulates the Proliferation and Differentiation of Prostate Epithelial Progenitor Cells

P5 mouse VPs were cultured for 48 hr in an organotypic culture system with 10 μM carbachol or 10 μM darifenacin prior to the following experiments.

(A) Organotypic cultures of VPs demonstrated that activation of ACS by carbachol (10 μM) promoted prostatic branching morphogenesis, whereas inhibition of ACS by darifenacin (10 μM) inhibited prostatic branching morphogenesis. Scale bar, 1 mm.

(B) Statistical analysis of bud number by counting the branching tips in each prostate (n = 10 different VPs).

(C and D) Activation of muscarinic receptors increased the percentage of p63 (red) and EdU (green) double-positive proliferating epithelial progenitor cells. Data were collected by calculating the percentage of EdU^+ cells in $p63^+$ basal cells or $p63^-$ luminal cells (n = 6 different VPs). Scale bar, 25 μm.

(E and F) Co-immunostaining of basal cell marker CK5 (red) and luminal cell marker CK8 (green) showing more basal cells among total epithelial cells in carbachol-treated prostates. Data were collected by counting the number of $CK5^+$ basal cells and $CK5^-CK8^+$ luminal cells in each duct (n = 5 different VPs). Scale bar, 25 μm.

(G and H) Flow cytometry analysis of $EpCAM^+CK5^+$ positive basal cells in total $EpCAM^+$ epithelial cells (n = 3 experiments).

Data above were analyzed with Student's t test. *p < 0.05, **p < 0.01, ***p < 0.001. Error bars indicate the SEM.

show much difference between the epithelium and the stroma. In sharp contrast, *Chrm3* was more abundant in the epithelium than in the mesenchyme (Figure 1F). Immunofluorescent staining also confirmed the epithelium-specific expression of *Chrm3* in P5 mouse VP sections (Figure 1G). All these data demonstrate the presence of acetylcholine, ChAT, VAChT, and muscarinic receptors in the developing mouse prostate epithelium. Consistent with our previous study that identified the existence of ACS in human prostate epithelial cancer cells, these findings together suggest that there is an ACS in the developing mouse prostate epithelium.

ACS Regulates the Proliferation and Differentiation of Epithelial Progenitor Cells in Prostate Postnatal Development

To investigate the possible functions of ACS in regulating prostate postnatal development, we performed organotypic cultures as previously described, as a convenient working system (Leong et al., 2008; Wang et al., 2008). To validate the organotypic cultures, we compared the expression patterns of ACS molecules in freshly dissected tissues versus the organotypic cultures. As shown in Figures S1C and S1D, we found that the cellular expression pattern of CHRM3 and ChAT in the 2-day organotypic cultures was the same as freshly dissected prostate tissues (Figures 1B and 1G). Real-time PCR analysis also demonstrated that the expression of cholinergic-signaling-related genes remained unchanged (Figure S1E). These data validate that the organotypic culture system is reliable to study the roles of ACS in regulating prostate postnatal development.

For organotypic cultures, postnatal day 5 (P5) mouse VPs were isolated and cultured in the presence of 10 μM muscarinic receptor agonist carbachol. The branching morphogenesis was analyzed by counting the number of branching tips. We found that activation of muscarinic receptors by carbachol promoted prostatic branching morphogenesis (Figures 2A and 2B). Next, we wanted to study whether blockade of ACS also affected prostatic branching morphogenesis. Since the expression of *Chrm3* was significantly higher in the epithelial cells than in the mesenchymal cells (Figure 1F), we treated the isolated VPs with darifenacin, a selective CHRM3 antagonist. We found that inhibition of CHRM3 by darifenacin effectively reduced the formation of new buds (Figure 2B). In addition, we examined the

effects of AFDX-384, a specific antagonist for CHRM2 and CHRM4, on prostatic branching morphogenesis. As *Chrm2* and *Chrm4* were more abundant in the mesenchyme than in the epithelium, compared with the control group, AFDX-384 did not significantly affect prostatic branching morphogenesis (Figures S2A and S2B). In the organotypic cultures of dorsal-lateral prostate, we also confirmed that carbachol and darifenacin promoted or inhibited prostatic branching morphogenesis, respectively (Figures S2C and S2D). These data suggest that ACS regulates prostate development through CHRM3 that expressed on the epithelial cells.

To understand how ACS affects epithelial cell proliferation and differentiation and whether it exerts its effect via influencing the proliferation of epithelial progenitor cells, we co-stained EdU with a basal cell marker, p63. We found that carbachol promoted the proliferation of both basal cells and luminal cells, whereas darifenacin inhibited the proliferation of epithelial cells (Figures 2C and 2D). To examine the differentiation of epithelial progenitor cells, we performed dual immunostaining for basal cell marker CK5 and luminal cell marker CK8. We counted the number of basal cells and luminal cells in each duct. Compared with the control group, we observed more $CK5^+$ basal cells in carbachol-treated VPs and less $CK5^+$ basal cells in darifenacin-treated VPs (Figures 2E and 2F). Intriguingly, the number of luminal cells in each duct did not change significantly (Figure 2F). Given that luminal cells can be derived from either the proliferation of luminal cells or the differentiation of basal cells (Wang et al., 2014), the unchanged total number of luminal cells supports the idea that activation of ACS enhances basal cells by promoting basal cell proliferation and inhibiting the differentiation of basal progenitor cells. One plausible interpretation is that the reduction in the number of luminal cells that are differentiated from basal cells matches the enhanced number of luminal cells due to increased luminal cell proliferation, which leads to an unchanged total number of luminal cells.

In addition, we performed unbiased flow cytometry analysis to measure the percentage of $CK5^+$ basal cells in $EpCAM^+$ total epithelial cells. Similarly, flow cytometry analysis showed a higher percentage of basal cells in carbachol-treated VPs and less basal cells in darifenacin-treated VPs (Figures 2G and 2H). Consistently, we detected a higher level of *Krt5* mRNA in carbachol-treated cultures (Figure S3A). Moreover, examination of the expression levels of *Mki67* and cell cycle promoter *Ccnd1* also showed results in accordance with the proliferating status of VPs in different groups (Figure S3B). These data together indicate that ACS affects prostate postnatal development through regulating the proliferation and differentiation of epithelial progenitor cells.

Lineage Tracing Assay Confirms that ACS Regulates the Differentiation of Epithelial Progenitor Cells

Lineage tracing analysis using specific transgenic mouse lines is a useful tool to study the differentiation of prostate epithelial progenitor cells (Blackwood et al., 2011; Blanpain and Simons, 2013; Ousset et al., 2012; Wang et al., 2014). We performed lineage tracing of CK14-expressing basal cells to verify the regulation of ACS on the differentiation of epithelial progenitor cells (Figures 3A and 3B). VPs were dissected from P5 CK14-CreERT/Rosa26-RFP mice and cultured as described above. To activate CreERT, isolated VPs were incubated with 100 nM 4-hydroxytamoxifen (4-OHT) for 12 hr (Sato et al., 2009). The addition of 4-OHT can induce Cre activity in the nucleus and label the CK14 expressing cells with RFP (Wang et al., 2014). Thirty-six hours after the induction, we observed that RFP only labeled $CK5^+$ basal cells (Figure 3C). Then, we treated these VPs with carbachol or darifenacin for 48 hr. Forty-eight hours after the treatment, we performed frozen sectioning and co-stained the tissue sections with RFP and a basal cell marker, CK5. We observed both RFP^+CK5^+ basal cells and RFP^+CK5^- luminal cells in the tissue sections (Figure 3D), and we considered RFP^+CK5^- luminal cells as differentiated cells that originated from the RFP-labeled basal cells based on the RFP-lineage marker. We analyzed the percentage of RFP^+CK5^- cells over the total RFP-labeled cells and found that carbachol decreased the percentage of RFP^+CK5^- luminal cells, whereas darifenacin increased the percentage of RFP^+CK5^- luminal cells (Figures 3E and 3F). These results further confirm that ACS regulates the differentiation of prostate epithelial progenitor cells.

Knockdown of *Chrm3* Promotes the Differentiation of Epithelial Progenitor Cells in Renal Capsule Tissue Recombination Assays

To further examine the effects of ACS on epithelial cell differentiation in vivo, we carried out the renal capsule recombination assay, which is a useful model to examine the differentiation of epithelial progenitor cells (Cunha, 1973; Xin et al., 2003). We sorted the epithelial cells from P5 mouse VPs with Lin^-EpCAM^+ (Figure 1E). Sorted epithelial cells were cultured in low-binding-surface 6-well plates and transfected with sh-*Chrm3* lentivirus (Figure 4A). Two days later, puromycin (2 μg/ml) was added to eliminate untransfected cells. The transfection efficiency was examined by western blot (Figure 4B). Successfully transfected epithelial cells were combined with rat urogenital sinus mesenchymal (UGSM) cells and engrafted under the renal capsule of BALB/c nude mice. Six weeks later, we collected the kidneys and found that knockdown of *Chrm3* obviously reduced the size and weight of the recombinants (Figures 4C and 4D). The epithelium-specific staining of RFP confirmed that the regenerated epithelial cells originated

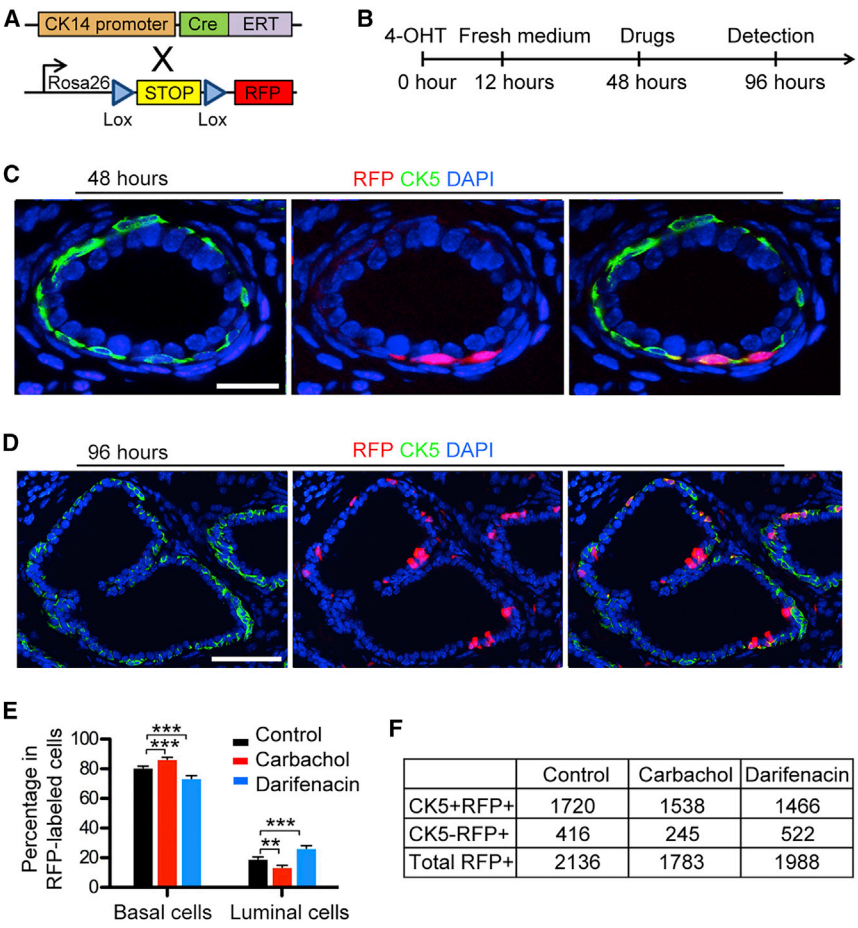

	Control	Carbachol	Darifenacin
CK5+RFP+	1720	1538	1466
CK5-RFP+	416	245	522
Total RFP+	2136	1783	1988

Figure 3. In Vitro Lineage Tracing Assay Confirms that ACS Regulates the Differentiation of Epithelial Progenitor Cells

(A and B) Schematic illustration and time course of the lineage tracing strategy.

(C) Co-immunostaining of RFP and basal cell marker CK5 (green) in VPs treated with 4-OHT for 48 hr. RFP only labeled $CK5^+$ basal cells. Scale bar, 50 μm.

(D) Co-immunostaining of RFP and basal cell marker CK5 (green) in VPs treated with 4-OHT for 96 hr. Note that genetically labeled RFP^+CK5^+ basal cells could differentiate to RFP^+CK5^- luminal cells. Scale bar, 100 μm.

(E and F) Statistical analysis of RFP^+CK5^- luminal cells over the total RFP-labeled cells. By counting cells from approximately 20 randomly acquired images from three different VPs, we had 2,136 RFP^+ cells in the control group, 1,783 RFP^+ cells in the carbachol group, and 1,988 RFP^+ cells in the darifenacin group. Note that compared with the control group, carbachol inhibited the differentiation of RFP-labeled basal cells, whereas darifenacin promoted the differentiation of basal cells.

Data above were analyzed with Student's t test. $^{**}p < 0.01$, $^{***}p < 0.001$. Error bars indicate the SEM.

from the implanted epithelial cells (Figure 4E). Immunofluorescent staining of CK5 and CK8 revealed that knockdown of *Chrm3* reduced the percentage of basal cells in total epithelial cells (Figure 4F). These findings indicate that inactivation of ACS promoted the differentiation of epithelial progenitor cells in vivo.

The Effects on Epithelial Progenitor Cells by ACS Are Achieved via Ca^{2+}/Calmodulin-Signaling-Mediated Phosphorylation of AKT

A common indicator for activation of ACS is calcium influx, as shown in prostate cancer cells (Wang et al., 2015b). To verify whether ACS also stimulated calcium influx in developing mouse prostate, we employed the Ca^{2+} indicator Fluo-4/AM to detect Ca^{2+} influx. Considering that small molecules were less permeable to tissues than monolayer cells, we increased the concentration of carbachol to 50 μM rather than 10 μM used in tissue cultures. In P3 VPs, the addition of carbachol obviously increased Ca^{2+} influx (Figures S4A and S4B), whereas suppression of CHRM3 by darifenacin largely decreased Ca^{2+} influx induced by carbachol (Figure S4C). In addition, inhibition of Ca^{2+}/calmodulin signaling by a calmodulin-specific antagonist N-(6-aminohexyl)-5-chloro-1-naphthalenesulfonamide hydrochloride (W-7, 5 μM) effectively inhibited the enhanced branching morphogenesis induced by carbachol (Figures 5A and 5B) in the organotypic prostate cultures. These data together indicate that ACS regulates prostate postnatal development through calcium singling.

To further confirm the involvement of Ca^{2+}/calmodulin signaling during ACS-regulated epithelial progenitor cell proliferation and differentiation, we performed immunofluorescent staining on tissue sections, which allows assessment of the detailed numbers of basal and luminal cells. The EdU incorporation assay showed decreased proliferating epithelial cells in W-7-treated cultures (Figures 5C and 5D). Co-immunofluorescent staining of CK5 and CK8 indicated that the addition of W-7 promoted the differentiation of progenitor cells into luminal cells (Figures 5E and 5F). Real-time PCR analysis also showed decreased *Krt5* mRNA expression in W-7-treated prostates (Figure S5A). Compared with carbachol-treated cultures, W-7 decreased the expression of *Mki67* and *Ccnd1* (Figure S5B).

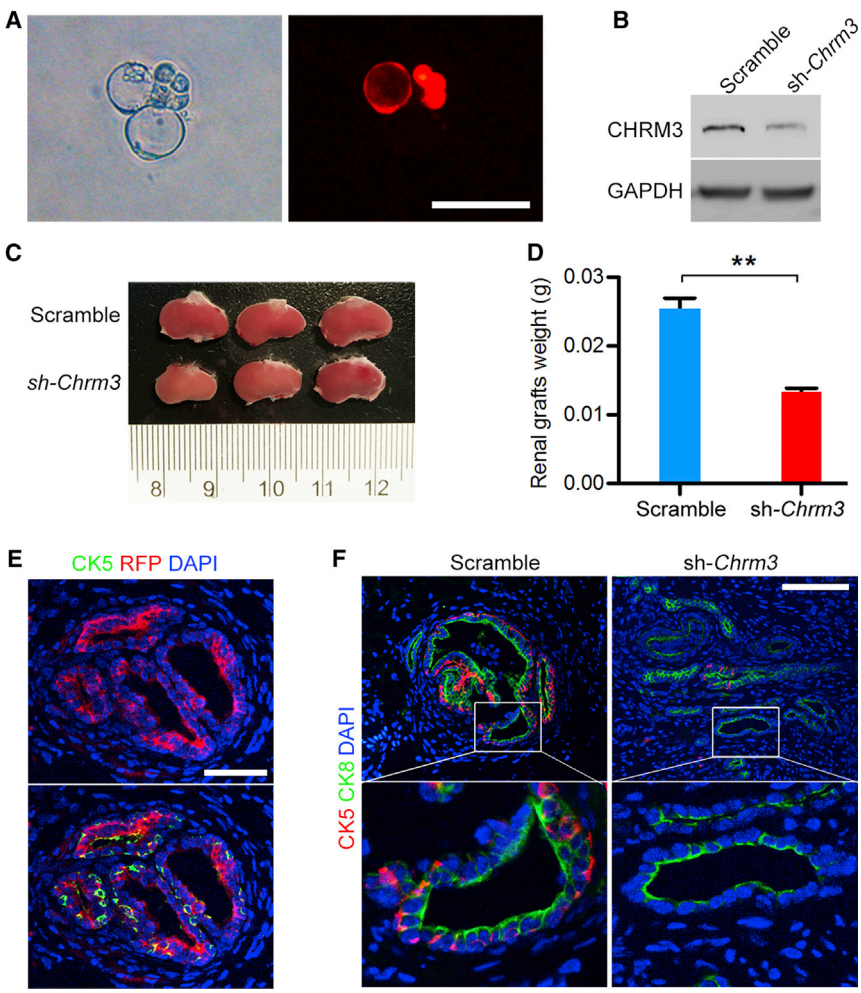

Figure 4. Knockdown of *Chrm3* Promotes the Differentiation of Epithelial Progenitor Cells in the Renal Capsule Tissue Recombination Assay

(A) Transfection of epithelial cells by scramble and sh-*Chrm3* lentivirus. Scale bar, 50 μm.

(B) Detection of CHRM3 knockdown efficiency by western blot.

(C) Renal capsule recombinants collected at 6 weeks.

(D) Knockdown of *Chrm3* decreased the weight of the recombined grafts (n = 6 grafts). Data were analyzed with Student's t test. **p < 0.01. Error bars indicate the SEM.

(E) Co-staining of RFP (red) and CK5 (green) confirmed that the regenerated epithelial cells originated from the implanted cells. Scale bar, 50 μm.

(F) Co-immunostaining of basal cell marker CK5 (red) and luminal cell marker CK8 (green). Scale bar, 100 μm.

To further confirm that ACS's regulation on the differentiation of epithelial progenitor cells is achieved via calcium signaling, we performed an ex vivo lineage tracing assay. We used VPs from CK14-CreERT/Rosa26-RFP mice and treated them with carbachol and W-7. We co-stained tissue sections with RFP and CK5 and found that blockade of calmodulin by W-7 increased the percentage of differentiated RFP^+CK5^- cells over the total RFP-labeled cells (Figure 5G), indicating that W-7 promoted the differentiation of epithelial progenitor cells. These results clearly indicate that ACS's regulation of prostate development is mediated through calcium signaling.

AKT, also known as protein kinase B (PKB), is a serine/threonine-specific protein kinase that plays a key role in the maintenance of epithelial progenitor cells. Continuous activation of AKT through the knockout of protein phosphatase and tensin homolog (PTEN) leads to increased epithelial progenitor cells in the prostate gland (Mulholland et al., 2009; Wang et al., 2006a) and the mammary gland (Korkaya et al., 2009). Since our previous study demonstrated that activation of ACS stimulated AKT phosphorylation in prostate cancer cells (Wang et al., 2015b), we next wanted to determine whether ACS regulates prostate development through regulating the phosphorylation of AKT. Immunofluorescent staining of phosphor-AKT (Ser473) indicated that AKT was abundantly activated in developing prostate epithelial cells (Figure S6). While carbachol stimulated the phosphorylation of AKT, both darifenacin and W-7 effectively reversed carbachol-induced AKT activation (Figures 5H and 5I). These results together suggest that ACS regulates prostate development and epithelial progenitor cell maintenance via Ca^{2+}/calmodulin-mediated phosphorylation of AKT.

Aberrant Activation of ACS Promotes Human BPH Cell Proliferation

To extend our findings from mouse prostate development to human prostate diseases such as BPH, we first wanted to identify the existence of ACS in normal human prostate epithelium. We performed immunostaining of TUJ1 and

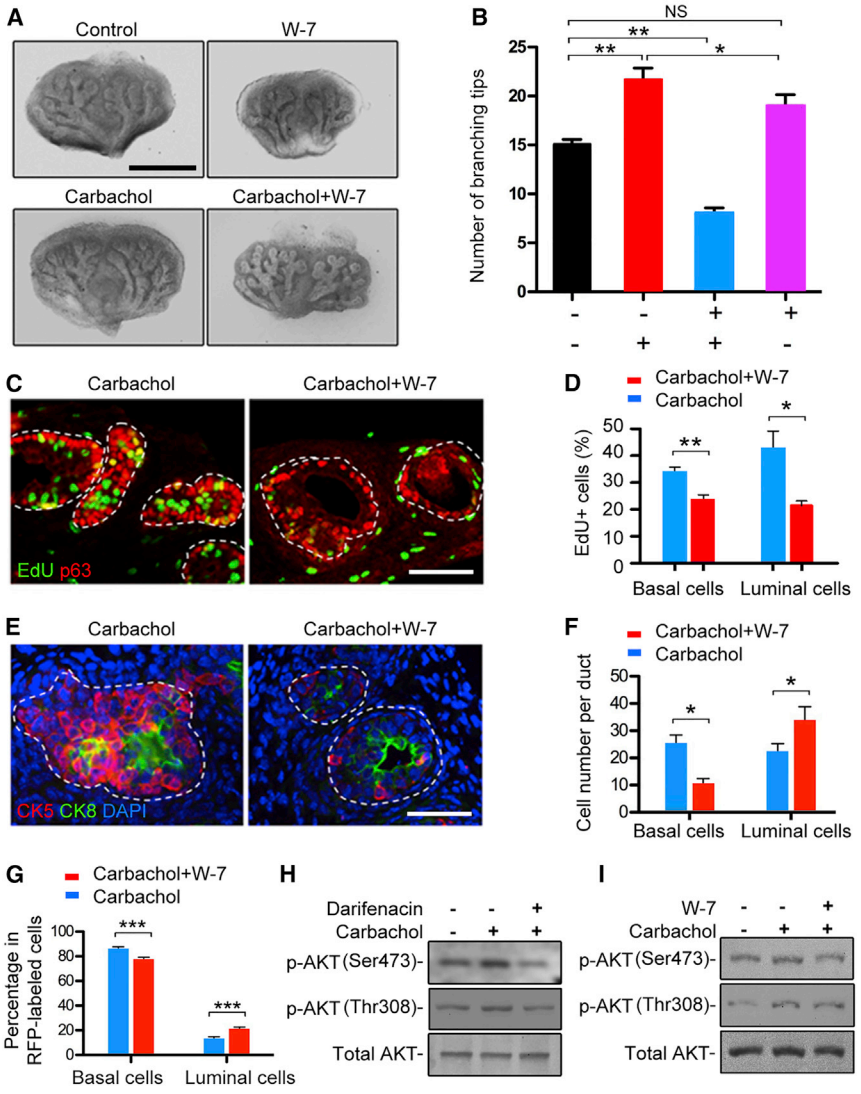

Figure 5. ACS Maintains the Proliferation and Differentiation of Epithelial Progenitor Cells in a CaM-Dependent Manner

(A–F) Mouse VPs were cultured for 48 hr in an organotypic system with 10 μM carbachol or 5 μM W-7 prior to the following experiments. (A) CaM inhibitor W-7 (5 μM) reduced branching morphogenesis induced by carbachol. Scale bar, 1 mm. (B) Statistical analysis of bud initiation in prostates with different treatments (n = 3 different VPs). (C and D) Co-immunostaining of p63 (red) and EdU (green) indicated that inhibition of CaM reduced the proliferation of basal cells induced by carbachol. The dashed lines depict the outlines of the epithelial cells. Quantification was performed by calculating the percentage of EdU^+ cells in $p63^+$ basal cells or $p63^-$ luminal cells (n = 3 different VPs). Scale bar, 50 μm. (E and F) Co-immunostaining of CK5 (red) and CK8 (green) showed that W-7 could reduce the number of basal cells in total epithelium. Data were collected by counting the number of $CK5^+$ basal cells and $CK5^-CK8^+$ luminal cells in each duct (n = 3 different VPs). Scale bar, 50 μm.

(G) Compared with the carbachol group (245/1783 RFP^+ cells), W-7 (367/1731 RFP^+ cells, n = 3 different VPs) decreased the percentage of $CK5^+$ cells in the total RFP-labeled cells.

(H and I) Western blotting analysis of AKT activation in cultured VPs. While carbachol increased the phosphorylation of AKT, both darifenacin and W-7 could effectively block the carbachol-induced activation of AKT.

Data above were analyzed with Student's t test. *$p < 0.05$, **$p < 0.01$, ***$p < 0.001$. Error bars indicate the SEM.

ChAT in normal human prostate tissue sections. As shown in Figure 6A, human prostate epithelial cells were not directly innervated by $TUJ\text{-}1^+$ nerve fibers, however, the epithelial cells showed strong ChAT immunoreactivity. Because our previous study had confirmed that CHRM3 played an important role in ACS-mediated prostate cancer growth and castration resistance, we compared mRNA expression of *CHRM3* in normal and BPH human prostate samples. We found that the expression of *CHRM3* varied little among normal prostate samples (Figure 6B). Compared with normal samples, however, the expression of *CHRM3* was upregulated in a large subset of the BPH samples (15 of 22 samples). Of the 15 samples in which *CHRM3* was upregulated, ten showed enhanced *CHRM3* expression with more than 5-fold changes (Figure 6B).

Next, we wanted to explore the consequence of disordered ACS in human BPH. We first detected calcium influx in BPH1 cells and found that blockade of CHRM3 by darifenacin could inhibit carbachol-induced calcium influx (Figure 6C). In addition, we examined the effects of ACS on the proliferation of human BPH1 cells, a transformed, non-tumorigenic cell line derived from human BPH tissue (Hayward et al., 1995). Whereas carbachol stimulated BPH1 cell proliferation, both darifenacin and W-7 counteracted the enhanced cell proliferation induced by carbachol (Figure 6D). Furthermore, we found that both darifenacin and W-7 also effectively inhibited the phosphorylation of AKT stimulated by carbachol (Figure 6E). These findings together suggest that aberrant activation of ACS promotes BPH

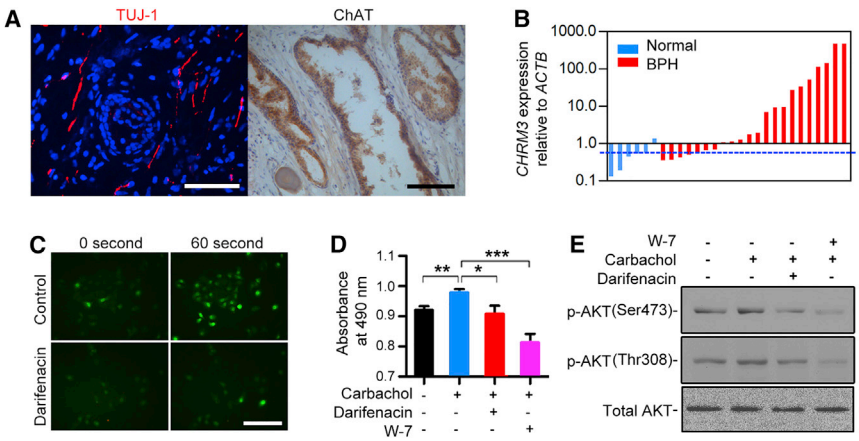

Figure 6. Aberrant Activation of ACS Promotes BPH Cell Proliferation via Ca^{2+}/Calmodulin Signaling-Dependent Phosphorylation of AKT

(A) Immunostaining of TUJ1 and ChAT in normal human prostate tissue sections. Scale bar, 100 μm.

(B) Real-time PCR analysis of *CHRM3* in clinical normal prostate samples (n = 6) and BPH samples (n = 22). The blue dotted line shows average expression levels of *CHRM3* in the normal prostate samples.

(C) Detection of calcium influx by Fluo-4 AM in BPH1 cells. Carbachol (10 μM) was used to trigger calcium influx. To counteract calcium influx, darifenacin (10 μM) was added 5 min before the stimulation of carbachol. Scale bar, 200 μm.

(D) Detection of cell proliferation by MTS in BPH1 cells. Carbachol stimulated BPH1 cell proliferation, while both darifenacin and W-7 counteracted the enhanced cell proliferation induced by carbachol (n = 3 experiments).

(E) Western blotting analysis of AKT activation in BPH1 cells. Both darifenacin and W-7 effectively inhibited AKT phosphorylation stimulated by carbachol. Cells were cultured in serum-free medium and stimulated by 10 μM carbachol for 5 min. In some samples, darifenacin (10 μM) or W-7 (5 μM) was added 1 hr before the stimulation of carbachol. Western blotting images were captured by Quantity One software.

Data above were analyzed with Student's t test. *$p < 0.05$, **$p < 0.01$, ***$p < 0.001$. Error bars indicate the SEM.

cell proliferation likely via calcium-signaling-mediated phosphorylation of AKT.

DISCUSSION

In this study, we identified the existence of non-neuronal ACS in developing prostate epithelium. Activation of ACS promoted the proliferation of epithelial progenitor cells and inhibited their differentiation to luminal cells. On the contrary, blockade of CHRM3 effectively inhibited the proliferation and promoted the differentiation of epithelial progenitor cells both in vitro and in vivo. In addition, we proved that ACS regulated prostate development and epithelial progenitor maintenance in a Ca^{2+}/calmodulin-signaling-dependent manner. Importantly, we found that CHRM3 was upregulated in a large subgroup of BPH human prostate samples. We further demonstrated that activation of CHRM3 promoted BPH cell proliferation through Ca^{2+}/calmodulin-signaling-mediated phosphorylation of AKT. Taken together, our study demonstrates an important role of non-neuronal ACS in the regulation of proliferation of prostate epithelial progenitor cells and BPH cells.

Although several signaling pathways have been reported to regulate postnatal prostate epithelial development, including Notch, Hedgehog, Wnt, and FGF signaling (Shen and Abate-Shen, 2010; Wang et al., 2003, 2006b, 2008, 2015a), the present study add ACS to the list. On the one hand, similar to other pathways such as Wnt (Wang et al., 2008), activation of ACS increases the percentage of basal epithelial cells by promoting proliferation and inhibiting differentiation of basal cells. On the other hand, different from other pathways, activation of ACS also promotes the proliferation of luminal cells. We further explored the mechanism of ACS in regulating prostatic development and found that ACS likely promotes proliferation of epithelial cells via calcium-signaling-mediated phosphorylation of AKT. It would be interesting in future studies to determine whether there are interactions between the ACS and these other signaling pathways.

It is important to point out that we performed ex vivo cell lineage tracing experiments with CK14-CreERT/Rosa26-RFP mice to study the differentiation of epithelial progenitor cells. Initially, activation of Cre by 4-OHT only labeled $CK5^+$ basal cells. However, after 2 days in culture, there appeared RFP^+CK5^- differentiated luminal cells that originated from the RFP^+ basal cells. Then we analyzed the percentage of RFP^+CK5^- cells over the total RFP-labeled cells under different culture conditions. We found that carbachol decreased the percentage of RFP^+CK5^- cells over the total RFP^+ cells, indicating that carbachol inhibited the differentiation of epithelial progenitor cells. On the contrary, darifenacin and W-7 increased the percentage of RFP^+CK5^- differentiated cells. These findings reinforce the notion that ACS regulates the differentiation of prostate epithelial progenitor cells.

BPH, an important clinical prostate disease, is a common prostatic disorder in elderly men. An estimated 40% of men aged ≥50 years and >90% of men aged ≥80 years have microscopic histopathological evidence of BPH (McNicholas and Kirby, 2011). However, at present, the cellular and molecular pathology of BPH is still poorly understood, and better clinical treatment is desired. In the present study, our findings provided a potential molecular mechanism for hyperplasia of the epithelial components of BPH. We found that CHRM3 was upregulated in a large subset of BPH samples. Activation of CHRM3 promoted BPH1 cell proliferation through promoting Ca^{2+}/calmodulin-signaling-dependent phosphorylation of AKT. Together with our previous study reporting an involvement of ACS in prostate cancer growth and castration resistance (Wang et al., 2015b), these findings indicate that aberrant activation of ACS also promotes BPH cell proliferation and suggest a potential application of a selective CHRM3 antagonist in the treatment of prostate diseases, including not only prostate cancer but also BPH.

EXPERIMENTAL PROCEDURES

Organotypic Cultures of Mouse VPs

Organotypic cultures were performed as previously described (Leong et al., 2008). VPs were dissected from postnatal day 5 (P5) mice and placed on 5 μm isopore membrane filters (TMTP02500, Millipore) in serum-free medium containing DMEM/F12 (Gibco), 100 nM testosterone (T6147, Sigma), insulin-transferrin-sodium selenite media supplement (I-1884, Sigma), 2 mM glutamine, 100 units/ml penicillin, and 100 mg/ml streptomycin (Gibco). Carbachol (10 μM, Sigma), darifenacin (10 μM, Santa Cruz Biotechnology), or W-7 (5 μM, Sigma) was added into the medium at the beginning of the culture. In some cultures, EdU (10 μM, Thermo Fisher) was added into the medium 1 hr before fixation. Tissues were fixed with 4% paraformaldehyde for 30 min on ice, washed in PBS, and then placed in 30% sucrose before processed for frozen sectioning. Animal studies were approved and carried out following the guidelines of Renji Hospital Institutional Animal Care and Ethics Committee.

Acetylcholine Detection

Acetylcholine concentration was measured using a choline/acetylcholine fluorometric kit (K615, BioVision) according to the manufacturer's instructions. P5 mouse VPs were isolated and cultured for 2 days, then weighed, and lysed in 100 μl of choline assay buffer by supersonic homogenizer before detection. Samples were measured by fluorescence at Ex/Em = 535/590 nm in a micro-plate reader.

Cell Sorting and Flow Cytometry Analysis

P5 mouse VPs were first cut into small pieces and digested in collagenase (1 mg/ml) for 1 hr at 37°C. After centrifuging, the pellets were collected and digested with 0.25% trypsin-EDTA for 10 min to dissociate the epithelial cells. The following primary antibodies were applied in cell sorting: CD45-fluorescein isothiocyanate (CD45-FITC) (#11-0451, eBioscience), TER119-FITC (#11-5921, eBioscience), CD31-FITC (#11-0311, eBioscience), EpCAM-PE-cy7 (#25-5791, eBioscience). Unstained samples, EpCAM-PE-Cy7-stained samples, and lineage-marker-stained samples were used as negative controls for compensation and FACS gating. Cells were sorted using a BD FACSAria II machine. To analyze $CK5^+$ basal cells within the $EpCAM^+$ total epithelial cells, enzymatically separated cells were first incubated with EpCAM-PE-Cy7 antibody (5 μl per test). Tubes were wrapped in aluminum foil and placed at room temperature for 30 min. After washing in PBS three times, cells were fixed with 4% paraformaldehyde (10 min) and permeabilized in PBS containing 0.5% Triton X-100 (10 min). Then rabbit CK5 antibody (PRB-160P, Covance) was added and incubated for 30 min at room temperature. Cells were washed three times in PBS, prior to incubation with FITC-conjugated goat anti-rabbit secondary antibody (Jackson ImmunoResearch) (30 min at room temperature). Flow cytometry analysis was performed on the BD FACSAria II machine.

Renal Capsule Tissue Recombination Assay

UGSM dissociation and renal capsule tissue recombination were performed as previously described (Leong et al., 2008). Sorted Lin^-EpCAM^+ prostate epithelial cells were cultured in low-attaching 6-well plates and transfected with CHRM3 short hairpin RNA (shRNA) lentivirus and scrambled shRNA lentivirus. The sequence of shRNA for *Chrm3* was 5′-CCG AGC CAA ACG AAC AAC AAA-3′. The transfection efficiency was determined by western blot analysis. Two days after the transfection, 2 μg/ml puromycin was added to select the successfully transfected epithelial cells. In each graft, 2,000 epithelial cells were combined with 250,000 UGSM cells. The samples were prepared in the following order (ten samples): 10× PBS (10 μl), 1 N NaOH (1.15 μl), collagen (50 μl, Corning), cell mixture (38.85 μl in PBS). The samples were incubated at 37°C for 1 hr to allow collagen gelation and overlaid with warm culture medium overnight at 37°C in a cell incubator. The samples were grafted under the renal capsule of 8-week-old male BALB/c nude mice. The grafts were harvested 6 weeks after the implantation.

Ex Vivo Lineage Tracing Assay

CK14-CreERT mice (#J006331) were obtained from Nanjing Biomedical Research Institute of Nanjing University. Rosa26-RFP mice were obtained from the Jackson Laboratory (#007914). To activate CreERT, isolated VPs were incubated with 4-hydroxytamoxifen (100 nM, Sigma) for 12 hr (Sato et al., 2009). Tissues were recovered in fresh organ culture medium for 36 hr before treatment with carbachol and darifenacin.

Immunofluorescent Staining

For fluorescent staining of cultured mouse prostate tissues, 6–8 μm frozen sections were stained with primary antibodies including CK5 (SIG-3475 and PRB-160P, Covance), CK8 (MMS-162P, Covance), CHRM3 (#251652, Abbiotec; sc-9108, Santa Cruz), p63 (sc-8431, Santa Cruz), Ki67 (ab16667, Abcam), TUJ-1 (T2200, Sigma), RFP (PM005, MBL) and ChAT (MAB305, Millipore). The primary antibodies were visualized with Alexa Fluor 488 or 594 conjugated secondary Fab fragment antibodies (Jackson ImmunoResearch). Fluorescent images were taken using a Leica DM2500 microscope.

Clinical Sample

Six normal human prostate samples were obtained from bladder cancer patients. Twenty-two BPH samples were collected from puncture biopsies. The pathological condition of the BPH samples was determined by experienced urologists at Ren Ji Hospital. All prostate samples were obtained from Ren Ji Hospital and collected with patients' informed consent.

SYBR Green Real-Time PCR

Total RNA was obtained and reversed to cDNA using the RNeasy plus Mini Kit and QuantiTect RT Kit (Qiagen). Real-time PCR was performed using SYBR green PCR reagents from Takara. Real-time PCR was performed on 7900HT PCR system (ABI). Thermal cycle conditions included 10 min at 95°C to activate DNA polymerase, 40 cycles of 95°C for 5 s, and 60°C for 30 s. Primer sequences are listed in Table S1.

Calcium Influx Detection

P3 VPs were anchored to the bottom of 24-well cell culture plates with 10 μl of Matrigel (354234, BD). Tissues were incubated with Fluo-4 AM (F-14201, Thermo Fisher, 2 μM in Hank's balanced salt solution) for 1 hr at 37°C and incubated for another 15 min in fresh HBSS to allow de-esterification of intracellular AM esters. Carbachol (50 μM) was used to induce Ca^{2+} influx, and 10 μM darifenacin was added 5 min before carbachol to suppress Ca^{2+} influx. Time-lapse images were taken with a Leica inverted microscope for 300 s with intervals of 6 s. Data were analyzed with Image-Pro Plus 6.0 software.

Cell Proliferation Detection

The proliferation of BPH1 cells was determined by CellTiter 96 AQueous One Solution Cell Proliferation Assay (MTS) (G3580, Promega). The experiments were performed following the manufacturer's instructions. Two thousand cells were seeded in 96-well plats and treated with carbachol, darifenacin, or W-7 for 24 hr. Twenty microliters MTS working solution was added and cultured in the incubator for 2 hr. Absorbance was detected at 490 nm.

Western Blot

Cells were lysed in a RIPA buffer (Thermo Fisher) with proteinase inhibitors (Calbiochem) and phosphatase inhibitors (Roche). The concentration of total proteins was measured by a BCA method (Thermo Fisher). Primary antibodies against CHRM3 (#251652, Abbiotec), ChAT (MAB305, Millipore), VAChT (BMP048, MBL), AKT (#4691), p-AKT (Ser473) (#4060), or p-AKT (Thr308) (#13038) (all AKT antibodies were purchased from Cell Signaling Technology) were applied, and the membranes were further processed with a horseradish peroxidase-conjugated secondary antibody (Jackson ImmunoResearch). Immunoblots were visualized with an ECL blotting detection kit (Thermo Fisher) and analyzed using Bio-Rad Quantity One software (version 4.1).

Statistical Analysis

Prostate epithelial branching morphogenesis was measured by counting the number of branching tips in each of the cultures. Organotypic cultures were repeated at least three times. All the statistical values were reported as means ± SEM. Quantification of immunofluorescent staining was performed by counting the number of positive cells in the total number of epithelial cells in fields from more than three different VPs. Results from real-time PCR and cell proliferation assays were analyzed using a non-parametric Student's t test. Statistical significance was defined as $^{*}p < 0.05$, $^{**}p < 0.01$, $^{***}p < 0.001$.

SUPPLEMENTAL INFORMATION

Supplemental Information includes six figures and one table and can be found with this article online at http://dx.doi.org/10.1016/j.stemcr.2016.04.007.

AUTHOR CONTRIBUTIONS

Naitao Wang planned the project, designed and performed the experiments; Bai-Jun Dong, Wei Xue, and Yi-Ran Huang provided the clinical prostate samples. Yizhou Quan and Mingliang Chu assisted in the establishment of the organotypic culture system; Qianqian Chen assisted in part of the immunofluorescent staining. Jin Xu performed the FACS analysis; Wei-Qiang Gao and Ru Yang conceived the ideas, planned and supervised the project; Naitao Wang and Wei-Qiang Gao wrote the manuscript.

ACKNOWLEDGMENTS

The study is supported by funds to W-Q.G. from the Chinese Ministry of Science and Technology (2012CB966800, 2013CB945600, and 2012CB967903), the National Natural Science Foundation of China (81130038 and 81372189), the Science and Technology Commission of Shanghai Municipality (Pujiang program), the Shanghai Education Committee Key Discipline and Specialty Foundation (J50208), the Shanghai Health Bureau Key Discipline and Specialty Foundation, and the KC Wong foundation.

Received: July 3, 2015
Revised: April 8, 2016
Accepted: April 8, 2016
Published: May 10, 2016

REFERENCES

Blackwood, J.K., Williamson, S.C., Greaves, L.C., Wilson, L., Rigas, A.C., Sandher, R., Pickard, R.S., Robson, C.N., Turnbull, D.M., Taylor, R.W., et al. (2011). In situ lineage tracking of human prostatic epithelial stem cell fate reveals a common clonal origin for basal and luminal cells. J. Pathol. *225*, 181–188.

Blanpain, C., and Simons, B.D. (2013). Unravelling stem cell dynamics by lineage tracing. Nat. Rev. Mol. Cell Biol. *14*, 489–502.

Chua, C.W., Shibata, M., Lei, M., Toivanen, R., Barlow, L.J., Bergren, S.K., Badani, K.K., Mc Kiernan, J.M., Benson, M.C., Hibshoosh, H., et al. (2014). Single luminal epithelial progenitors can generate prostate organoids in culture. Nat. Cell Biol. *16*, 951–961.

Cunha, G.R. (1973). The role of androgens in the epithelio-mesenchymal interactions involved in prostatic morphogenesis in embryonic mice. Anat. Rec. *175*, 87–96.

Goldstein, A.S., Huang, J.T., Guo, C.Y., Garraway, I.P., and Witte, O.N. (2010). Identification of a cell of origin for human prostate cancer. Science *329*, 568–571.

Hayward, S.W., Dahiya, R., Cunha, G.R., Bartek, J., Deshpande, N., and Narayan, P. (1995). Establishment and characterization of an immortalized but non-transformed human prostate epithelial cell line: BPH-1. In Vitro Cell. Dev. Biol. Anim. *31*, 14–24.

Karthaus, W.R., Iaquinta, P.J., Drost, J., Gracanin, A., van Boxtel, R., Wongvipat, J., Dowling, C.M., Gao, D., Begthel, H., Sachs, N., et al. (2014). Identification of multipotent luminal progenitor cells in human prostate organoid cultures. Cell *159*, 163–175.

Korkaya, H., Paulson, A., Charafe-Jauffret, E., Ginestier, C., Brown, M., Dutcher, J., Clouthier, S.G., and Wicha, M.S. (2009). Regulation of mammary stem/progenitor cells by PTEN/Akt/beta-catenin signaling. PLoS Biol. *7*, e1000121.

Landgraf, D., Barth, M., Layer, P.G., and Sperling, L.E. (2010). Acetylcholine as a possible signaling molecule in embryonic stem cells: studies on survival, proliferation and death. Chem. Biol. Interact. *187*, 115–119.

Lawson, D.A., Xin, L., Lukacs, R.U., Cheng, D., and Witte, O.N. (2007). Isolation and functional characterization of murine prostate stem cells. Proc. Natl. Acad. Sci. USA *104*, 181–186.

Leong, K.G., Wang, B.E., Johnson, L., and Gao, W.Q. (2008). Generation of a prostate from a single adult stem cell. Nature *456*, 804–808.

McNicholas, T., and Kirby, R. (2011). Benign prostatic hyperplasia and male lower urinary tract symptoms (LUTS). Clin. Evid. *2011*, 1801.

Mulholland, D.J., Xin, L., Morim, A., Lawson, D., Witte, O., and Wu, H. (2009). Lin-Sca-1+CD49fhigh stem/progenitors are tumor-initiating cells in the Pten-null prostate cancer model. Cancer Res. *69*, 8555–8562.

Ousset, M., Van Keymeulen, A., Bouvencourt, G., Sharma, N., Achouri, Y., Simons, B.D., and Blanpain, C. (2012). Multipotent and unipotent progenitors contribute to prostate postnatal development. Nat. Cell Biol. *14*, 1131–1138.

Sato, T., Vries, R.G., Snippert, H.J., van de Wetering, M., Barker, N., Stange, D.E., van Es, J.H., Abo, A., Kujala, P., Peters, P.J., et al. (2009). Single Lgr5 stem cells build crypt-villus structures in vitro without a mesenchymal niche. Nature *459*, 262–265.

Serobyan, N., Jagannathan, S., Orlovskaya, I., Schraufstatter, I., Skok, M., Loring, J., and Khaldoyanidi, S. (2007). The cholinergic system is involved in regulation of the development of the hematopoietic system. Life Sci. *80*, 2352–2360.

Shen, M.M., and Abate-Shen, C. (2010). Molecular genetics of prostate cancer: new prospects for old challenges. Genes Dev. *24*, 1967–2000.

Shou, J., Ross, S., Koeppen, H., de Sauvage, F.J., and Gao, W.Q. (2001). Dynamics of notch expression during murine prostate development and tumorigenesis. Cancer Res. *61*, 7291–7297.

Spindel, E.R. (2012). Muscarinic receptor agonists and antagonists: effects on cancer. In Muscarinic Receptors, A.D. Fryer, A. Christopoulos, and N.M. Nathanson, eds. (Springer), pp. 451–468.

Takahashi, T., Ohnishi, H., Sugiura, Y., Honda, K., Suematsu, M., Kawasaki, T., Deguchi, T., Fujii, T., Orihashi, K., Hippo, Y., et al. (2014). Non-neuronal acetylcholine as an endogenous regulator of proliferation and differentiation of Lgr5-positive stem cells in mice. FEBS J. *281*, 4672–4690.

Wang, B.E., Shou, J.Y., Ross, S., Koeppen, H., de Sauvage, F.J., and Gao, W.Q. (2003). Inhibition of epithelial ductal branching in the prostate by sonic hedgehog is indirectly mediated by stromal cells. J. Biol. Chem. *278*, 18506–18513.

Wang, S., Garcia, A.J., Wu, M., Lawson, D.A., Witte, O.N., and Wu, H. (2006a). Pten deletion leads to the expansion of a prostatic stem/progenitor cell subpopulation and tumor initiation. Proc. Natl. Acad. Sci. USA *103*, 1480–1485.

Wang, X.D., Leow, C.C., Zha, J.P., Tang, Z.J., Modrusan, Z., Radtke, F., Aguet, M., de Sauvage, F.J., and Gao, W.Q. (2006b). Notch signaling is required for normal prostatic epithelial cell proliferation and differentiation. Dev. Biol. *290*, 66–80.

Wang, B.E., Wang, X.D., Ernst, J.A., Polakis, P., and Gao, W.Q. (2008). Regulation of epithelial branching morphogenesis and cancer cell growth of the prostate by Wnt signaling. PLoS One *3*, e2186.

Wang, X., Kruithof-de Julio, M., Economides, K.D., Walker, D., Yu, H.L., Halili, M.V., Hu, Y.P., Price, S.M., Abate-Shen, C., and Shen, M.M. (2009). A luminal epithelial stem cell that is a cell of origin for prostate cancer. Nature *461*, 495–500.

Wang, J., Zhu, H.H., Chu, M., Liu, Y., Zhang, C., Liu, G., Yang, X., Yang, R., and Gao, W.Q. (2014). Symmetrical and asymmetrical division analysis provides evidence for a hierarchy of prostate epithelial cell lineages. Nat. Commun. *5*, 4758.

Wang, B.E., Wang, X., Long, J.E., Eastham-Anderson, J., Firestein, R., and Junttila, M.R. (2015a). Castration-resistant lgr5(+) cells are long-lived stem cells required for prostatic regeneration. Stem Cell Rep. *4*, 768–779.

Wang, N., Yao, M., Xu, J., Quan, Y., Zhang, K., Yang, R., and Gao, W.Q. (2015b). Autocrine activation of CHRM3 promotes prostate cancer growth and castration resistance via CaM/CaMKK-mediated phosphorylation of Akt. Clin. Cancer Res. *21*, 4676–4685.

Wessler, I.K., and Kirkpatrick, C.J. (2012). Activation of muscarinic receptors by non-neuronal acetylcholine. Handb. Exp. Pharmacol., 469–491.

Xin, L., Ide, H., Kim, Y., Dubey, P., and Witte, O.N. (2003). In vivo regeneration of murine prostate from dissociated cell populations of postnatal epithelia and urogenital sinus mesenchyme. Proc. Natl. Acad. Sci. USA *100* (*Suppl 1*), 11896–11903.